Articles

Mechanisms of Mutagenesis by Exocyclic DNA Adducts. Construction and in Vitro Template Characteristics of an Oligonucleotide Bearing a Single Site-Specific Ethenocytosine†

Devendranath Simha, Vaseem A. Palejwala, and M. Zafri Humayun*
Department of Microbiology and Molecular Genetics, University of Medicine and Dentistry of New Jersey-New Jersey Medical School, 185 South Orange Avenue MSB F607, Newark, New Jersey 07103-2714
Received April 17, 1991; Revised Manuscript Received June 26, 1991

ABSTRACT: By using a gene-targeted random DNA adduction approach, we have recently shown that chloroacetaldehyde, a metabolite of vinyl chloride, induces mutations predominantly at cytosines under conditions in which both ethenoadenine (εA) and ethenocytosine (εC) are formed. Although the observed mutational specificity of εC suggested that it was a noninstructional lesion, the high efficiency of mutagenesis and an apparent lack of SOS dependence were reminiscent of mispairing lesions. To obtain more direct evidence showing that εC has properties of a noninstructional mutagenic lesion, we have examined the in vitro template properties of a single εC residue at a unique position in a synthetic oligonucleotide. The oligonucleotide was constructed by use of the following steps: (a) in vitro treatment of the pentameric oligodeoxyribonucleotide TTCTT with chloroacetaldehyde to convert the central cytosine to ethenocytosine; (b) purification and characterization of TTεCTT; and (c) ligation of purified TTεCTT to two decamers to create a 25 nt long oligodeoxyribonucleotide with a centrally located εC residue. The template characteristics of εC were examined by the annealing of end-labeled primers to the purified εC-containing oligonucleotide and primer elongation by *Escherichia coli* DNA polymerase I in the presence of one or more nucleotide precursors. The elongation products were analyzed by high-resolution gel electrophoresis followed by autoradiography and quantitated by computing densitometry. The results indicated the following: (a) at low nucleotide precursor concentrations at which guanine incorporation can be readily demonstrated opposite normal cytosine, no detectable base incorporation occurs opposite εC; (b) base incorporation opposite εC can be detected in the presence of relatively high concentrations of nucleotide precursors; adenine is preferentially incorporated, followed by thymine, whereas guanine and cytosine are poorly incorporated. These results establish that εC lesions display the in vitro template properties expected of noninstructional lesions. However, in this experimental system, continued synthesis beyond the εC site is most efficient when the incorporated base is a thymine.

An increasing number of bifunctional chemical agents are now known to induce exocyclic DNA lesions. For example, the carcinogen vinyl chloride is activated by cellular metabolism to two bifunctional alkylating agents, the first being chloroethylene oxide (CEO).[1] CEO can suffer spontaneous (and rapid) rearrangement to form the second agent, chloroacetaldehyde (CAA; Guengerich et al., 1979). Both CEO and CAA react with DNA to induce the exocyclic ethenoadenine (εA), ethenocytosine (εC; Figure 1), and ethenoguanine lesions as well as other adducts [for reviews, see Barbin and Bartsch (1986) and Singer and Spengler (1986)]. Although interest in the possible mutagenic activity of etheno derivatives was stimulated relatively recently by the identification of low levels of etheno derivatives in the DNA and RNA and animals exposed to vinyl chloride (Green & Hathaway, 1978; Laib & Bolt, 1977; Eberle et al., 1989) and alkyl carbamates [e.g., Leithauser et al. (1990)], etheno derivatives are particularly well-studied examples of exocyclic DNA lesions because of their early use as enzyme substrate analogues and polynucleotide structural probes [see review by Leonard (1984); Kochetkov et al., 1971; Barrio et al., 1972; Shulman & Pelka, 1976; Biernat et al., 1978; Kusmierek & Singer, 1982; Kohwi-Shigematsu et al., 1983; Lilley, 1986; Jacobsen et al., 1987; Laib & Bolt, 1987; Vogt et al., 1988). The first hints that etheno derivatives may be potentially mutagenic came from studies on effects of etheno lesions in synthetic polynucleotide templates on in vitro replication or transcription. Surprisingly, however, while some studies found that thymine was preferentially incorporated opposite putative εC residues (Barbin et al., 1981; Singer et al., 1983), other studies found that adenine was the predominant misincorporated base (Hall et al., 1981).

Even though both CAA (McCann et al., 1975) and CEO (Barbin et al., 1985) were shown to induce reversion in bacterial systems, direct evidence implicating etheno lesions in mutagenesis has only recently been obtained (Jacobsen et al., 1989; Jacobsen & Humayun, 1990). In these experiments, etheno adduction was directed to a 178 nt long segment of the M13AB28 LacZ(α) gene by exploiting the known reaction

† This work was supported by USPHS Grant CA47234.
* Corresponding author.

[1] Abbreviations: CEO, 2-chloroethylene oxide; CAA, 2-chloroacetaldehyde; εC, 3,N^4-ethenocytosine; εA, 1,N^6-ethenoadenine; A, adenine; C, cytosine; G, guanine; T, thymine; polI(k) *E. coli* DNA polymerase I large (Klenow) fragment; polI(k)$^{exo-}$, mutant version of *E. coli* DNA polymerase I large fragment devoid of both 5′→3′ and 3′→5′ exonuclease activities; 25-mer^{εC}, a synthetic 25 nt long oligonucleotide bearing a single, centrally located εC residue; 25-mer^{C}, a control version of 25-mer^{εC} in which the εC residue has been replaced by normal cytosine.

0006-2960/91/0430-8727$02.50/0

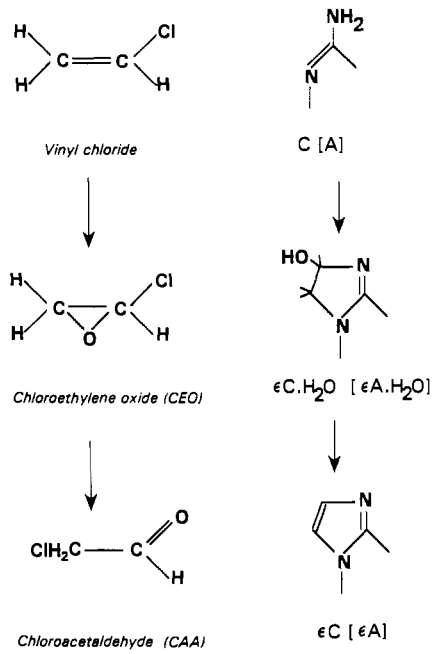

FIGURE 1: (Left) Chemical structures of vinyl chloride, 2-chloroethylene oxide (CEO), and 2-chloroacetaldehyde (CAA). CEO, the primary metabolic product of vinyl chloride, spontaneously and rapidly rearranges to CAA. Stuctures of a part of cytosine (or adenine) and the corresponding etheno derivatives (εC and εA) are shown on right (adapted from Krzyzosiak et al., 1986). Both CAA and CEO react with cytosine (or adenine) to yield εC (or εA) through the unstable hydrated intermediates εC·H_2O and εA·H_2O. Note that etheno bridging eliminates two of three Watson–Crick hydrogen-bonding positions of cytosine.

preference of CAA for single-stranded DNA. Both εC and εA were formed under these conditions, but evidence indicated that εC was highly mutagenic while εA was at best weakly mutagenic. The mutations attributable to εC were mostly C-to-T transitions followed by C-to-A transversions, a specificity indicative of noninstructional mutagenic lesions. Many noninstructional lesions are believed to be bypassed by the so-called "adenine rule", according to which DNA polymerase preferentially (but not exclusively) incorporates adenine opposite sites devoid of accessible template information [e.g., Rabkin & Strauss (1984), Kunkel (1984), Walker (1984), and Loeb and Preston (1986)]. That εC probably acts as a noninstructional lesion is also consistent with the fact that the etheno, bridging of cytosine (Figure 1) would disrupt two of three G·C Watson–Crick hydrogen bonds and that satisfactory alternative base-pairing capabilities are not known. Paradoxically, however, mutagenesis by εC lesions is apparently SOS independent, and highly efficient, two properties associated with miscoding rather than noninstructional lesions.

Since the observed properties could define εC as a novel type of mutagenic lesion, we have sought to obtain direct evidence to link the lesion with its previously deduced in vitro and in vivo properties. In this paper, we describe the construction, purification, and characterization of a 25 nt long oligodeoxyribonucleotide containing a single εC residue. This site-specifically modified oligonucleotide has been used in experiments designed to examine the relative efficiency with which various bases are inserted (or misinserted) opposite εC lesions and the efficiency of lesion bypass after each type of base incorporation.

Materials and Methods

Materials. All solvents and water used in biochemical manipulation of oligonucleotides were HPLC grade from Fisher. Most deoxyribonucleotide triphosphates were HPLC-purified grade from Pharmacia or were obtained as a generous gift from Dr. N. Sinha. Deoxyethenocytosine 3′-phosphate (dεCp), used as a marker in postlabeling analyses, was prepared as described (Jacobsen et al., 1989) and purified by HPLC. *Escherichia coli* DNA polymerase I large (Klenow) fragment [polI(k)] as well as a mutant version of the same enzyme lacking in both 3′→5′ and 5′→3′ exonuclease activities [polI(k)$^{exo-}$; double mutant D355A–E357A of Derbyshire et al. (1988)], purified to homogeneity, was a generous gift of Dr. M. Modak. Sources of other materials are indicated where appropriate below.

Oligonucleotide Synthesis and Purification. All oligonucleotides were synthesized by standard automated phosphoramidite technology on an Applied Biosystems Model 380A synthesizer. The oligonucleotides were deblocked and initially purified by cellulose thin-layer chromatography (solvent, 1-propanol/ammonium hydroxide/water 55:35:10). The oligonucleotides were subjected to further HPLC purification on a C18 column (Hewlett-Packard Hypersil ODS, 100 × 4.6 mm) with use of 100 mM triethylammonium acetate, pH 7/acetonitrile as described below. Purity was confirmed by end labeling and electrophoresis on high-resolution denaturing polyacrylamide gels. Primers used in this study were purified (after the initial TLC purification as above) by electrophoresis on preparative denaturing 20% polyacrylamide/8 M urea gels.

Chemical Modification of 5′-HO-TTCTT-OH to 5′-HO-TTεCTT-OH. The pentamer 5′-HO-TTCTT-OH (100–150 μg) was incubated with a 1000 molar excess of CAA (obtained from ICN-K & K laboratories as an aqueous 45% solution) in 200 μL of buffer (200 mM sodium cacodylate, pH 7) for 48 h at 37 °C. This treatment condition was found to convert >95% of the pentamer to 5′-HO-TTεCTT-OH. The reaction mix was diluted to 2 mL with water and purified on a Waters Sep-Pak C18 cartridge as follows. Before use, the cartridge was given one wash with acetonitrile (10 mL), two washes with water (10 mL each), and one wash with 10 mM ammonium acetate, pH 8 (2 mL). The reacted pentamer solution was loaded, and the cartridge was washed twice with water (10 mL each). The pentamer was eluted with three 1-mL portions of methanol/water (60:40). The eluates were pooled and evaporated to dryness under reduced pressure in a Savant SpeedVac machine. The pentamer residue was subjected to two cycles of resuspension in 100 μL of water and reevaporation as above. The final residue was suspended in 300 μL of water and the 5′-HO-TTεCTT-OH was purified by two sequential HPLC steps as described under Results.

Postlabeling Analysis. The procedures of Hollstein et al. (1986), based on the original work of Randerath et al. (1981), were followed as described (Jacobsen et. al., 1989). A total of 1 μg of the pentamer (or 200 ng of the 25-mer) was digested to nucleoside 3′-monophosphates (dNps) by incubation with 0.2 unit of spleen phosphodiesterase (Sigma) and 0.4 unit of micrococcal nuclease (Sigma) in 30 μL of 20 mM Tris-HCl (pH 6.8)/10 mM $CaCl_2$, for 4 h at 37 °C. (Both nucleases were extensively dialyzed against water at 4 °C before use.) Simultaneous 5′-^{32}P-labeling and 3′-phosphate removal were accomplished by incubating 500 pmol of nucleoside 3′-phosphates with 2 pmol of [γ-^{32}P]ATP (>5000 Ci/mmol) and 20 units of T4 polynucleotide kinase (New England Biolabs) in 20 μL of 50 mM Tris-HCl (pH 6.8)/10 mM $MgCl_2$/10 mM dithiothreitol for 1 h at 37 °C. (At pH 6.8, T4 kinase also removes 3′-phosphates.) The reaction was terminated by the addition of EDTA to 25 mM, and 2 μL (~50 pmol of nucleotides) was fractionated on PEI–cellulose plates (Sigma)

as described by Jacobsen et al. (1989).

5′-Phosphorylation of Oligonucleotides. The oligonucleotide (15 μg) was incubated with 1 mM ATP and 100 units of T4 polynucleotide kinase (New England Biolabs) in 100 μL of kinase buffer (50 mM Tris-HCl, pH 7.6, 10 mM $MgCl_2$, 5 mM DTT, 0.1 mM EDTA) for 60 min at 37 °C. The reaction was terminated by one phenol extraction followed by three ether extractions. The DNA was freed from excess ATP by Sep-Pak purification as described above or by filtration on a Sephadex G-10 "spun column" as described in standard laboratory manuals. Under these conditions, 5′-phosphorylation of pentameric and decameric oligonucleotides was complete as judged by subsequent polyacrylamide/urea gel electrophoresis and inspection of oligonucleotide bands by UV shadowing.

Construction of 25-mers. To construct 25-mers, 7 μg of purified 5′-pTTCTT-OH (control) or 5′-pTTεCTT-OH, 14 μg each of the 5′ decamer (5′-AATTGTGGAG) and the 3′ decamer (5′-pATCGTGTGCA), and 24 μg of the complementary 17-mer (5′-CACGATAAGAACTCCAC) in 30 μL of ligase buffer (50 mM Tris-HCl, pH 7.6, 10 mM $MgCl_2$, 10 mM DTT) were incubated at 55 °C for 30 min and slow-cooled overnight to 4 °C. Ligation was initiated by the addition of ATP (to 1 mM) and T4 DNA ligase (2000 New England Biolabs units; 60 vendor units = 1 Weiss unit) in a final volume of 50 μL of the above ligase buffer, and incubation was continued for 12 h at 4 °C (5′-pTTεCTT-OH) or for 2–3 h at 4 °C (5′-pTTCTT-OH). The reaction was terminated by phenol extraction, and excess ATP was removed by gel filtration on a Sephadex G-10 spun column. The major portion of the reaction mix was phosphorylated as described above. To generate gel markers, a small fraction of the ligation mix was phosphorylated in the presence of 50 μCi of [γ-^{32}P]ATP (>5000 Ci/mmol; Amersham) as above and chased for 15 min with 1 mM unlabeled ATP. The phosphorylated ligation products were fractionated on 25% polyacrylamide/8 M urea gels together with labeled markers, and the 25-mer product was recovered from the gel by standard procedures. The recovered oligonucleotide was freed from small molecules by two cycles of ethanol precipitation and was quantitated by spectrophotometry.

Preparation of Primed Templates and DNA Elongation Assays. A total of 1 nmol of the appropriate synthetic oligonucleotide primer (3–4 μg) containing 5′OH and 3′OH groups was 5′-end-labeled by incubation for 60 min at 37 °C with T4 polynucleotide kinase (50 units; New England Biolabs) in the presence of 150 μCi of [γ-^{32}P]ATP (>5000 Ci/mmol; Amersham) and 20 pmol of unlabeled ATP (final specific activity: ~3000 Ci/mmol) in 50 μL of the above kinase buffer. The reaction was terminated by phenol extraction, and the primer was freed from small molecules by Sephadex G-10 spun column chromatography. The recovered oligonucleotide was quantitated by UV absorption in a spectrophotometer. A total of 25 pmol of the εC-containing 25-mer (25-mer$^{\epsilon C}$) or the control cytosine-containing 25-mer (25-mer^{C}) were annealed with 12.5 pmol of the labeled primer in 50 μL of annealing buffer (50 mM Tris-HCl, 10 mM $MgCl_2$, 1 mM dithiothreitol, pH 7.8) by the following sequential steps: incubation at 70 °C for 10 min, slow-cooling to room temperature over 2–3 h, followed by slow-cooling overnight (6–16 h) to 4 °C in a refrigerator. Typical elongation reactions were carried out at 23 °C in 40–60 μL of the annealing buffer (except for the addition of 100 μg/mL bovine serum albumin; Sigma) containing 0.5 pmol of primed template per 10 μL (i.e., 1 pmol of template and 0.5 pmol of primer per 10 μL of the reaction mix), 1 ng (~15 fmol) of the indicated DNA polymerase, one or more dNTP(s) in concentrations ranging from 1 μM to 1 mM for 1–10 min. Aliquots (10 μL) were withdrawn at the indicated time intervals, mixed with 10 μL of a formamide/dye stop solution (0.25% each of bromphenol blue and xylene cyanole in formamide), and set on ice until the completion of each experiment. The contents were heated at 90 °C for 3 min and immediately chilled to 0 °C, and 2 μL was loaded on 16% polyacrylamide/8 M urea thin (sequence) gels and fractionated at 1500 VDC for 3–5 h. Autoradiography was carried out by exposing Kodak XRP-1 film to the gel for 12–24 h as necessary for densitometric analysis (see below).

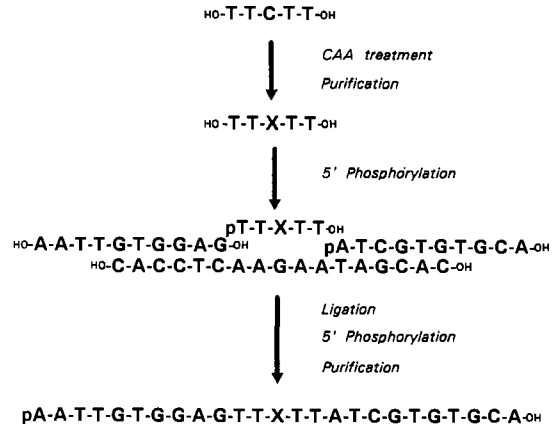

FIGURE 2: Strategy for incorporating a single εC lesion at a unique position within a 25 nt long synthetic oligodeoxyribonucleotide. A pentamer consisting of a single centrally located cytosine residue and four thymines is treated in vitro with CAA. The modified pentamer containing εC in place of C is purified and ligated with two decamers in the presence of a complementary scaffolding 17-mer to obtain a 25-mer containing a centrally located εC.

Densitometric Analysis. Percent primer elongation, defined below, was calculated on the basis of a densitometric analysis of autoradiographs. The total autoradiographic signal contained in each band in each lane was determined by using a Molecular Dynamics Model 300B computing densitometer employing the volume integration method, with appropriate corrections for background absorption. For example, the 12-mer elongation products shown in Figure 8 (top autoradiograph) are quantitated as follows (see lane 8 [dATP/6′] of Figure 8 as an example). A grid consisting of a stack of two rectangular cells of unequal height is positioned over the primer and the three product bands such that all bands in the lane are entirely contained within the grid. (The column width is set to slightly exceed the width of the bands). The primer (or precursor) band is boxed by the bottom (short) cell of the grid, while all three product bands are boxed by the upper (tall) cell of the grid. The total signal (minus background) contained in each cell is computed by volume integration. Percent elongation is determined as

$$\text{percent elongation} = \frac{\text{signal in product bands}}{\text{signal in product and precursor bands}} \times 100$$

Autoradiographic exposure conditions are selected to be within the linear film response range.

Results

Strategy for Construction of a 25-mer Bearing a Single εC Residue. The strategy, outlined in Figure 2, consists of (a) in vitro adduction of the pentamer 5′-HO-TTCTT-OH with CAA; (b) purification and characterization of the εC-con-

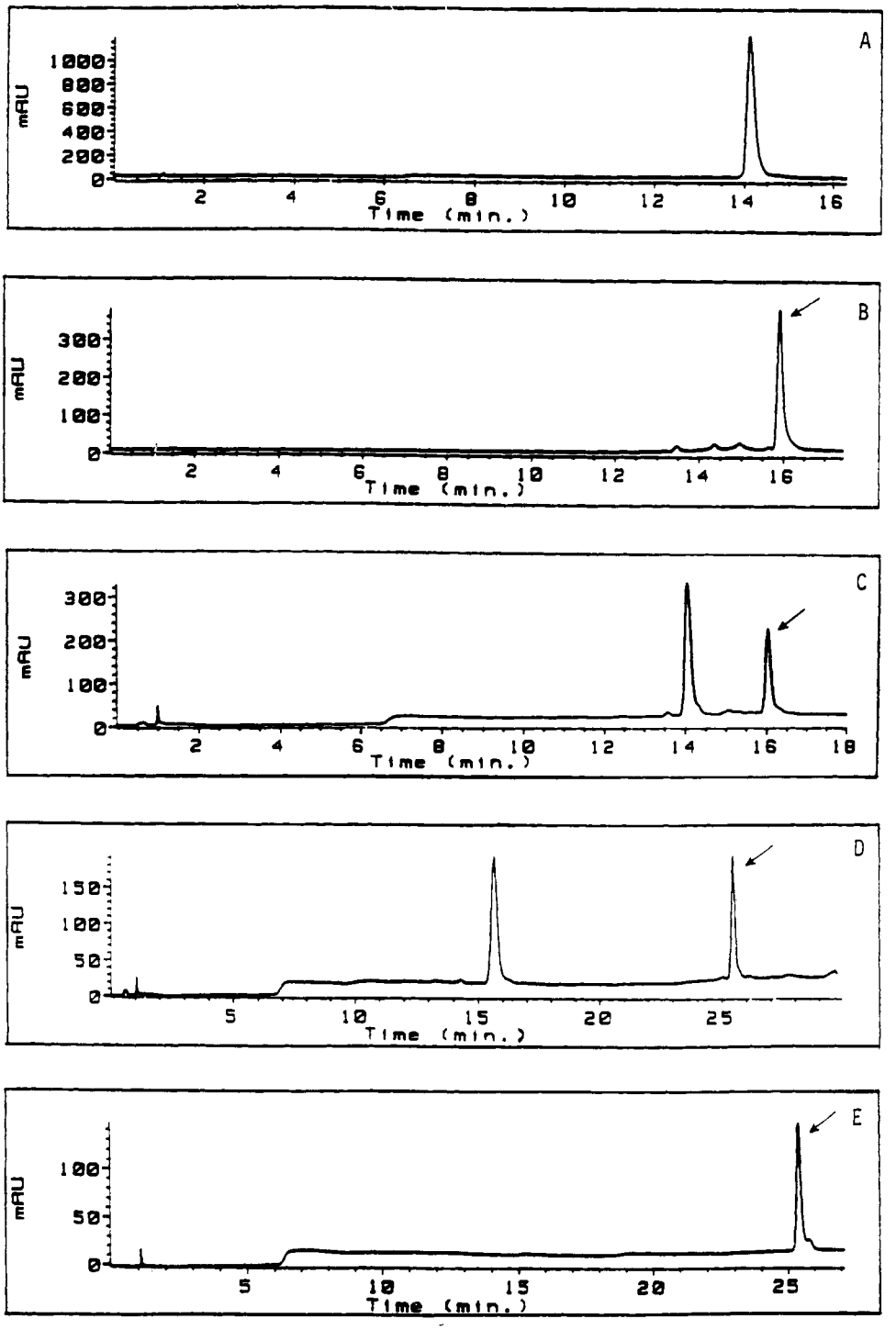

FIGURE 3: HPLC purification of 5′-HO-TTεCTT-OH. The following solvents were used: solvent A, 100 mM triethylammonium acetate, pH 7; solvent B: 30% acetonitrile in 100 mM TEAA. (Panels A–C) Elution program I: 0–100% B in 30 min. (Panels D–E) Elution program II: 0–32% B in 10 min; 32% B for 10 min; 32–70% B 10 min. (Panel A) The untreated pentamer 5′-HO-TTCTT-OH, eluting at 14 min (peak 1). (Panel B) The CAA-treated pentamer. Note the putative εC-containing pentamer eluting at 16 min (peak 2, marked with arrow in all panels). (Panel C) A 1:1 mix of the treated and untreated pentamers to confirm the identities of peak 1 and 2. (Panel D) Profile of a similar mix using elution program II. (Panel E) Final purification (using program II) of material shown in panel B. mAU, milli absorbance unit.

taining derivative 5′-HO-TTεCTT-OH; (c) 5′-phosphorylation of the pentamer to obtain 5′-pTTεCTT-OH; (c) incorporation of the pentamer into a 25-mer by ligation with a 5′- (left) decamer and a 3′- (right) decamer in the presence of a complementary 17-mer (scaffold); and (d) purification of the 25-mer by denaturing polyacrylamide gel electrophoresis.

Preparation and Characterization of 5′-pTTεCTT-OH. Figure 3 shows the HPLC elution profile of the pentamer 5′-HO-TTCTT-OH before (panel A) and after (panel B) in vitro adduction with CAA as described. It can be seen that CAA treatment converts more than 95% of the pentamer to a later eluting (more hydrophobic) species. To confirm that the material eluting at 16 min is not the starting pentamer, treated and untreated pentamers were mixed and fractionated. The results (panel C) showed that the added untreated pentamer eluted earlier and confirmed that CAA treatment does indeed yield a pentamer with increased hydrophobicity. To examine whether the late eluting pentamer contained εC in

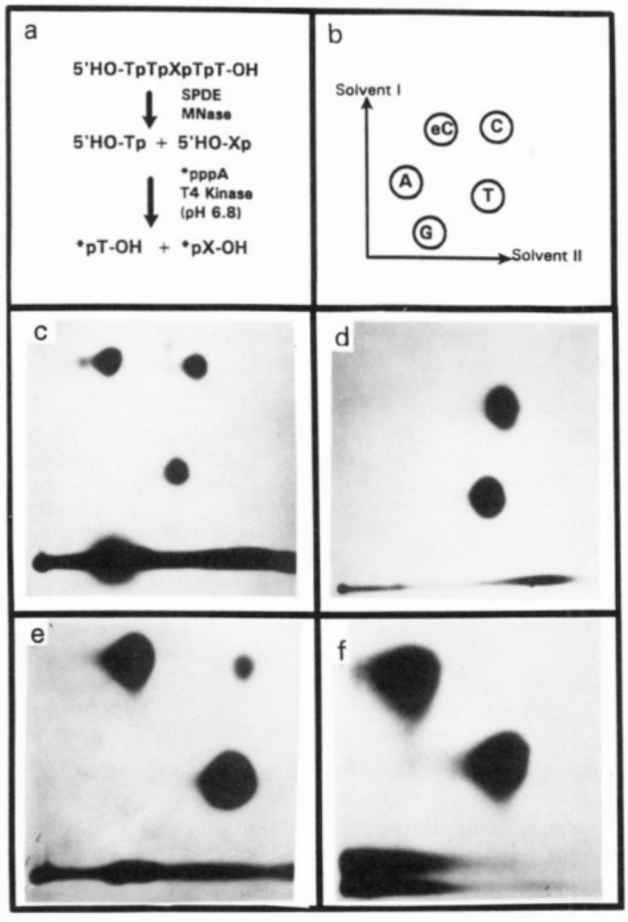

FIGURE 4: Postlabeling analysis of untreated and CAA-treated pentamer (5′-HO-TTCTT-OH). Procedures were as described by Jacobsen et al. (1989). (Panel a) Summary of procedures used in postlabeling. SPDE, spleen phosphodiesterase; MNase, micrococcal nuclease; *pppA, [γ-^{32}P]ATP (see Materials and Methods for details). (Panel b) Diverging arrows with the labels solvent I (1 M ammonium acetate, pH 3.5) and solvent II (3.75 M ammonium sulfate, pH 3.5) indicate the directions of the first and second fractionation steps as previously described (Jacobsen et al., 1989). The approximate positions of various deoxyribonucleoside 5′-monophosphates (dpN) are indicated. (Although G and A are not present in the digests in this procedure, their positions are marked for comparison.) (Panel c) Postlabeled artificial mix of dϵCp, dCp, and dTp to generate labeled markers corresponding to dpϵC, dpC, and dpT. (Panel d) Untreated pentamer, showing dpC and dpT. (Panel e) Treated pentamer after first HPLC purification (see Figure 3B, peak marked with arrow). Note persisting low levels of dpC indicating contamination of 5′-HO-TTϵCTT-OH with 5′-HO-TTCTT-OH. (Panel f) Treated pentamer after second HPLC purification (see Figure 3E, peak marked with arrow) showing the presence of dpϵC and dpT but no dpC.

place of C, the untreated pentamer and the treated, HPLC-purified pentamer were subjected to postlabeling analysis as described (Figure 4, panel a). In this particular type of postlabeling analysis, DNA (or oligonucleotides) are digested with nucleases to nucleoside 3′-phosphates (dNp). The dNp mix is incubated with T4 polynucleotide kinase in the presence of [γ-^{32}P]ATP under conditions (pH 6.8) that permit 5′-phosphorylation of the nucleotides with simultaneous removal of the 3′-phosphate by the 3′-nucleotidase activity of the enzyme, ultimately yielding 5′-^{32}P-labeled deoxyribonucleoside 5′-monophosphates (dpN). Figure 4c shows the results of two-dimensional fractionation of an artificial mix of authentic radiolabeled dpT, dpC, and dpϵC to indicate the positions of the respective nucleotides. Figure 4d represents the postlabeling analysis of untreated pentamer. The autoradiograph, as expected, shows spots corresponding to dpT and dpC. Figure 4e shows that the material eluting at 16 min (see Figure 3B) yields dpT and dpϵC, confirming that it represents the ϵC-bearing pentamer. However, Figure 4e also shows that a minor spot corresponding to dpC is present, indicating that the purified pentamer is most likely contaminated with small amounts of unmodified (C-containing) pentamer. To further purify the 5′-HO-TTϵCTT-OH pentamer, the material was subjected to a second cycle of HPLC purification using a combination of gradient and isocratic elution methods (Figure 3D,E). The material eluting at 25 min under the conditions described (Figure 3E), when analyzed by postlabeling (Figure 4f), showed the presence of dpT and dpϵC, but no dpC. To confirm the autoradiographic observations, the spots corresponding to dpϵC as well as the blank area corresponding to the expected position of dpC were cut out and subjected to scintillation counting. This analysis confirmed that the adducted pentamer, isolated as described above, was >99% pure. The purified 5′-HO-TTϵCTT-OH was phosphorylated with T4 polynucleotide kinase to obtain 5′-pTTϵCTT-OH and was used in this form in all subsequent steps.

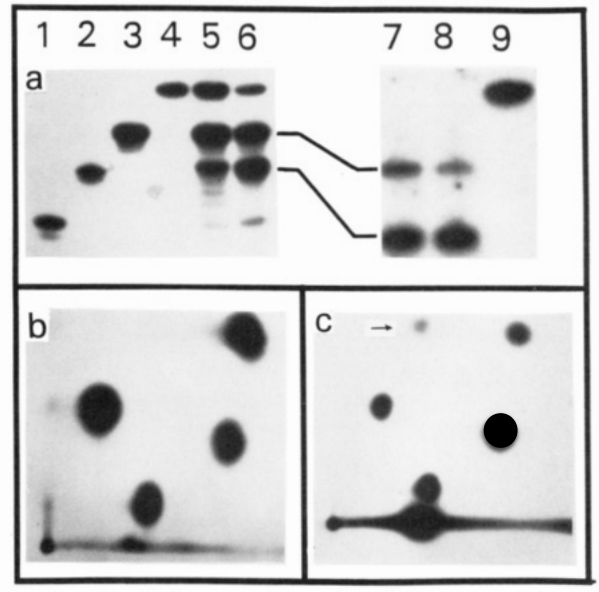

FIGURE 5: (Panel a) Autoradiographs of denaturing 25% polyacrylamide gels where 5′-end-labeled products of ligation of 5′-pTTϵCTT-OH (or of 5′-pTTCTT-OH) with two decamers were fractionated. For strategy and procedures, see Figure 2 and Materials and Methods. Lanes 1–4, size markers (5, 10, 17, and 25 nt); lane 5, 3-h ligation of 5′-pTTCTT-OH to produce the control (cytosine-containing) version of the 25-mer (25-mer^{C}); lane 6, 12-h ligation of 5′-pTTϵCTT-OH to produce the site-specifically modified 25-mer (25-mer$^{\epsilon C}$). Note the lower level of ligation for 5′-pTTϵCTT-OH (lane 6) despite the longer ligation time. Lane 7 (no pentamer) and lane 8 (pTTϵCTT-OH present, but no DNA ligase) are controls, while lane 9 is a 25-mer marker. (Panels b and c) Postlabeling analysis of 25-mer^{C} (b) and of 25-mer$^{\epsilon C}$ (c). See Figure 4 and Materials and Methods for procedures and the identity of the spots shown. Note that ϵC is present only in the 25-mer$^{\epsilon C}$ digest (panel c, arrow).

Construction and Characterization of the 25-mer. In order to construct a single-stranded 25-mer containing a centrally placed ϵC lesion, the 5′-pTTϵCTT-OH prepared as above was ligated with a 5′-phosphorylated 3′-decamer and a 5′-hydroxyl-bearing 5′-decamer in the presence of a complementary 17-mer that served as a scaffold (see Figure 2 for sequences). Figure 5a shows autoradiographs of gels on which ligation products that were 5′-end-labeled with ^{32}P were fractionated. These data show that the ligation of the control pentamer (5′-pTTCTT-OH; lane 5) to yield the 25-mer^{C} is efficient (up to 90% ligation was observed by 3 h), whereas, presumably due to the decreased complementarity of 5′-pTTϵCTT-OH, its ligation to yield 25-mer$^{\epsilon C}$ (lane 6) is much

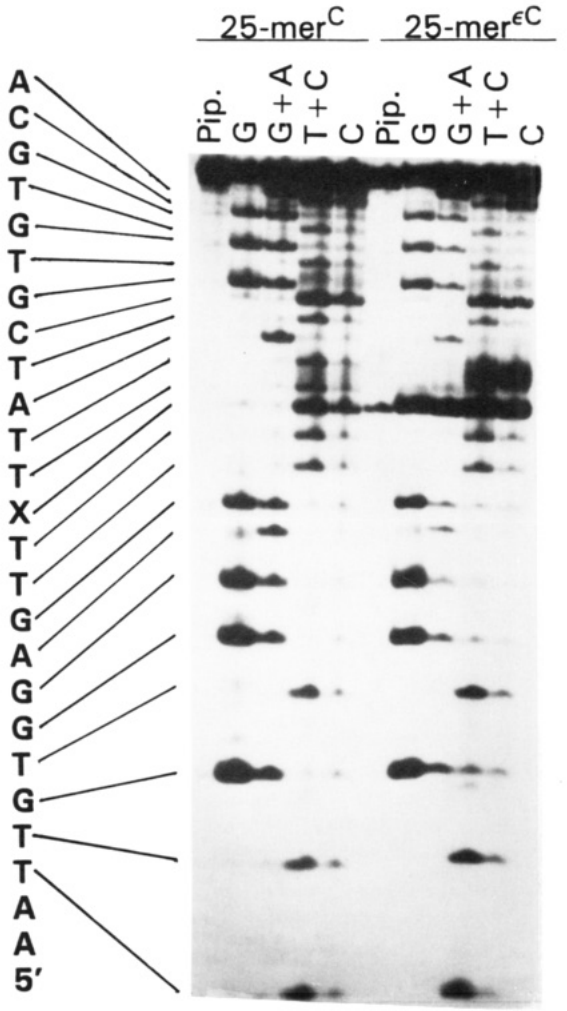

FIGURE 6: Maxam–Gilbert chemical degradation analysis of 25-mer^{C} and 25-mer$^{\epsilon C}$. Reactions were carried out as described in Sambrook et al. (1989). The sequence of bases 3–25 can be read in this autoradiograph. Because ϵC is alkali labile (Vogt et al., 1988), results with the 25-mer$^{\epsilon C}$ reveal uniform base degradation in all lanes at the sequence position X, including the lane (Pip) in which the 25-mer$^{\epsilon C}$ was directly subjected to piperidine cleavage. Degradation is not observed at this position for the 25-mer^{C} (X = C).

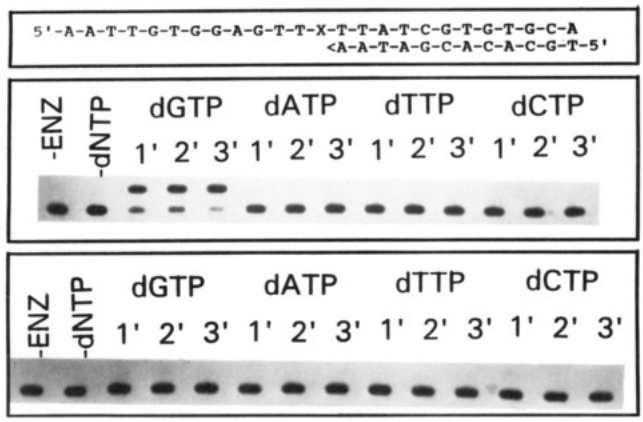

FIGURE 7: Autoradiographs showing the effect of ϵC on incorporation of various bases by exonuclease-deficient *E. coli* DNA polymerase I large fragment [polI(k)$^{exo-}$] at low (1 μM) dNTP concentrations. All elongation reactions were carried out as described under Materials and Methods ([dNTP] = 1 μM). The template (upper strand, 25-mer) and the primer (12-mer) sequences are shown in the upper panel. The middle panel shows the data for the normal template (25-mer^{C}; X = C) revealing substantial guanine incorporation within the first few minutes. (Incubation time is indicated in minutes above each lane.) The bottom panel shows that the modified template (25-mer$^{\epsilon C}$; X = ϵC) does not permit incorporation of any base under the same conditions. The lanes labeled –ENZ (no polymerase) and –dNTP (no nucleoside triphosphate) represent control elongation reactions.

less efficient (up to 20% by 12 h). The 25-mer products obtained in preparative-scale ligation reactions were phosphorylated at the 5′-end with nonradioactive phosphorus and gel-purified as described under Materials and Methods.

The following observations and experiments confirmed that the observed 25-mer was the correctly assembled product containing an ϵC residue. First, when the pentamer was omitted from the ligation reaction, no 25-mer was formed (Figure 5a, lane 7). Second, postlabeling analysis showed the presence of ϵC in the constructed 25-mer$^{\epsilon C}$ (Figure 5c, arrow), but not in the 25-mer^{C} (Figure 5b). Third, Maxam–Gilbert sequence analysis showed the sequence expected for the 25-mer (Figure 6). The ϵC residue (base X in the sequence shown) was heavily cleaved in all reactions due to the alkali lability of the lesion (Vogt et al., 1988; Figure 6, last 4 lanes). Finally, direct piperidine/heat cleavage (Figure 6, lanes labeled Pip) showed the presence of a single alkali-labile site in the 25-mer$^{\epsilon C}$ but not in the 25-mer^{C}.

Base Incorporation Opposite ϵC during in Vitro DNA Elongation by E. coli DNA Polymerase I. On the basis of results obtained by transfection of gene-targeted random adduction experiments, we have previously proposed that ϵC has the in vivo template properties of a noninstructional lesion. If ϵC does act as a noninstructional lesion, it is expected that ϵC will not template for any base under conditions at which normal cytosine would readily template for guanine. Furthermore, at conditions of bypass such as high dNTP concentrations, it should be possible to demonstrate incorporation of adenine, and less frequently, of other bases, opposite ϵC as observed for other noninstructional lesions.

We have examined the template properties of ϵC in a defined in vitro system in which a 5′-end-labeled oligonucleotide primer annealed to the 25-mer$^{\epsilon C}$ is elongated in the presence of a DNA polymerase, metal cofactor, and one or more deoxynucleoside triphosphates (dNTP). The elongation products are separated from the primer by high-resolution denaturing polyacrylamide gel electrophoresis, and the relative amounts are quantitated by computing densitometry. Similar approaches have been used to characterize the template characteristics of randomly adducted DNAs [e.g., Rabkin and Strauss (1984)] as well as of oligonucleotides bearing site-specific lesions [e.g., Randall et al. (1987)]. In the experiments described here we have used a mutant version of the *E. coli* DNA polymerase I (Klenow fragment) deficient in both 5′→3′ and 3′→5′ exonuclease activities (polI(k)$^{exo-}$; Derbyshire et al., 1988) as well as its wild-type counterpart, polI(k).

Figure 7 (bottom autoradiograph) shows that under conditions in which DNA synthesis must be initiated by the incorporation of a base opposite ϵC, no base incorporation is observed. Figure 7 (top autoradiograph) shows that under the same conditions, guanine is readily incorporated opposite normal cytosine. In the elongation reactions shown in Figure 7, a dNTP concentration of 1 μM was used. However, when the dNTP concentrations were increased to the millimolar range, base incorporation opposite ϵC could be observed (Figure 8, top autoradiograph). Quantitation of the relative incorporation of each dNTP as a function of elongation time (Figure 9, upper graph) showed that adenine is preferentially incorporated opposite ϵC, followed closely by thymine. Incorporation of guanine is inefficient, and that of cytosine is very low. These observations are consistent with the possibility that ϵC lesions act as noninstructional lesions.

In the above experiments, DNA synthesis must be initiated by the incorporation of a base opposite the ϵC lesion (see

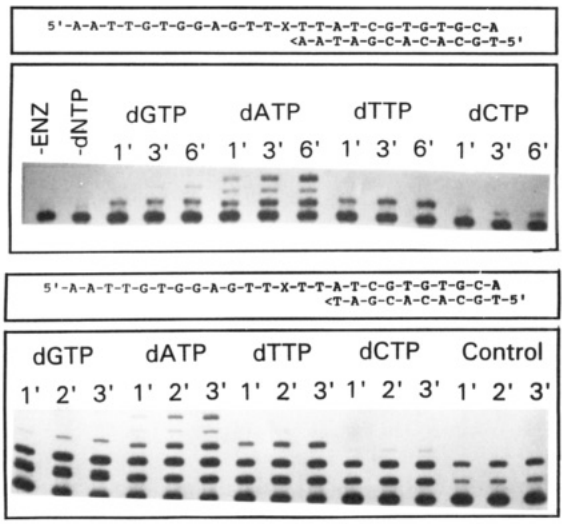

FIGURE 8: Autoradiographs showing the effect of ϵC on incorporation of various bases by polI(k)$^{exo-}$ at high (1 mM) dNTP concentrations. Modified template (X = ϵC) was used for all reactions shown. The top two panels show, respectively, the sequences of template–primer and the incorporation of various bases under conditions similar to those in Figure 7 except for the high dNTP (1 mM) concentrations used here. Note the relatively high incorporation of A and T, the lower incorporation of G, and the very poor incorporation of C. (In the presence of dATP, elongation continues for two more bases because the next two template bases are thymines. In the G reaction, in addition to the expected 13-mer product, a faint band indicating low levels of continued elongation is seen at 3 min. This is most likely due to misinsertion of G opposite T at high dGTP concentrations rather than due to contamination of dGTP with low levels of dATP.) The third panel (from top) gives the sequence of a different primer (a 10-mer) used to obtain the data shown in the bottom panel. The 10-mer primer initiates synthesis at the −2 position (i.e., two bases 3′ of base X on the template). These reactions were carried out as above except that all reactions had 1 μM dATP and, except for the control, all reactions additionally had the indicated dNTP at a concentration of 1 mM. In the bottom autoradiograph, note that the three shortest oligonucleotides (first three bands from the bottom; 10, 11, and 12 nt long; see control lanes) are precursors while the fourth band (13 nt) and up represent products arising from incorporation opposite (and elongation past) ϵC. Incubation time is indicated in minutes above each lane.

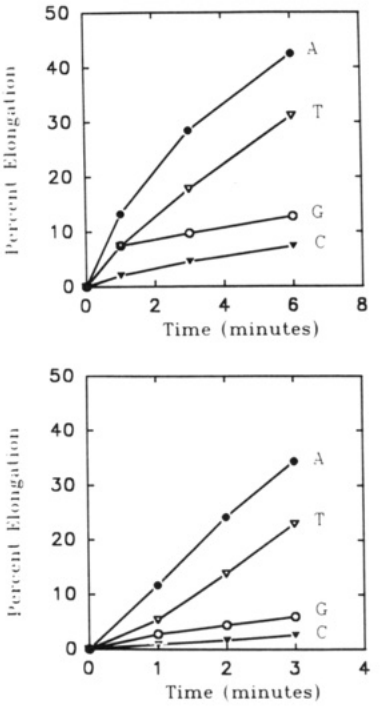

FIGURE 9: Incorporation of various bases opposite ϵC at high (1 mM) dNTP concentrations using the 12-mer primer (upper panel) or the 10-mer primer. See Figure 8 for template–primer sequences and reaction conditions. Percent elongation (relative amounts of 13–15 nt long products; see legend for Figure 8) is determined as described under Materials and Methods. The data shown are averages of two experiments.

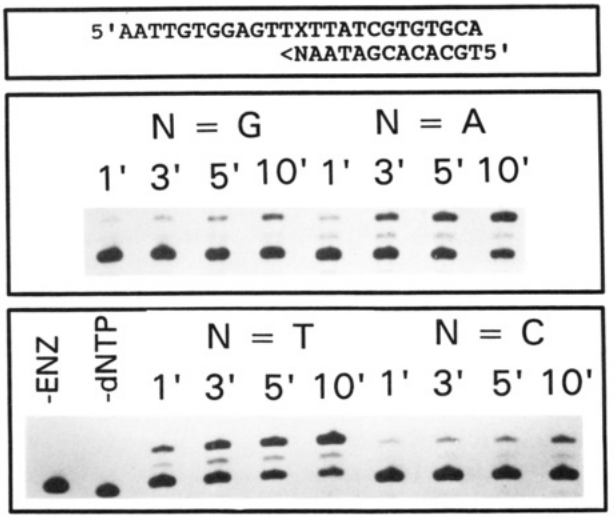

FIGURE 10: Autoradiographs showing the relative efficiency of elongation of each of the four bases incorporated opposite an ϵC residue in the template. Four 13-mer primers, differing only in the identity of the 3′-base (N in the primer sequence shown in the top panel), were used for each set of elongations. Reactions were carried out as described in Figure 7 except that all reactions (except the −dNTP control) had 20 μM dATP as the sole nucleoside triphosphate. PolI(k)$^{exo-}$ was used in these experiments. Incubation time is indicated in minutes above each lane.

Figure 8, top panel, for sequence). It is conceivable that the base incorporation preference observed under these conditions differs from that occurring during DNA elongation. To test this possibility, we annealed a shorter primer (a 10-mer) such that DNA synthesis is initiated two nucleotides 3′ of the ϵC site (Figure 8, bottom two panels). Since the two template bases preceding ϵC are thymines, in each of four separate reactions, 1 μM dATP was included along with a 1 mM concentration of the indicated dNTP. Under these conditions, in the absence of relatively high dNTP concentrations (see control in Figure 8, bottom autoradiograph), DNA synthesis terminates one nucleotide 3′ of the ϵC lesion: i.e., the 10-mer primer is elongated up to a 12-mer. In the presence of millimolar dNTP, base incorporation occurs opposite the lesion and elongation continues for an additional two bases beyond ϵC because of the availability of dATP. A quantitative analysis (Figure 9, bottom graph) indicates that under these conditions the base incorporation preference remains the same (i.e., A > T ≫ G > C) as that observed previously for the 12-mer primer. Therefore, ϵC lesions act as noninstructional lesions during DNA elongation as well as at the initiation of DNA synthesis.

Effect of the Base Incorporated Opposite ϵC on Continued Elongation past the Lesion. Among the factors that can influence mutational outcome is the efficiency of lesion bypass: i.e., the efficiency of continued elongation after base incorporation opposite the lesion. To test whether continued elongation past the ϵC lesion is equally efficient regardless of the identity of the incorporated base, we carried out the experiments described in Figure 10. Here, four different template–primers were created by annealing the 25-mer$^{\epsilon C}$ with four different 5′-end-labeled 13-mer primers. The primers differed from one another only in the identity of the 3′-terminal base, which was G, A, T, or C. Each template–primer com-

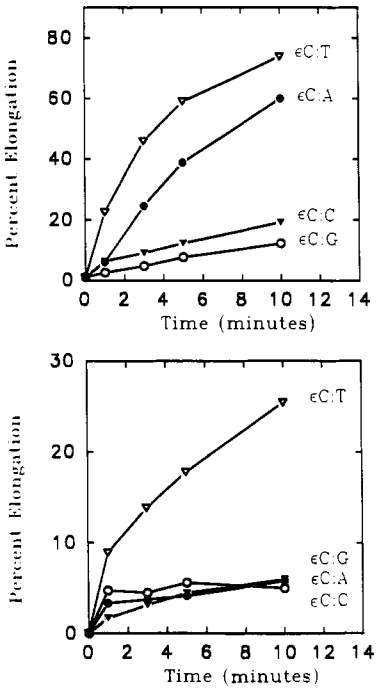

FIGURE 11: Elongation efficiency of various bases incorporated opposite εC using polI(k)$^{exo-}$ (upper panel) or wild-type polI(k) containing 3′→5′ exonuclease activity (lower panel). Percent elongation was determined as described under Materials and Methods. Values are averages for two experiments.

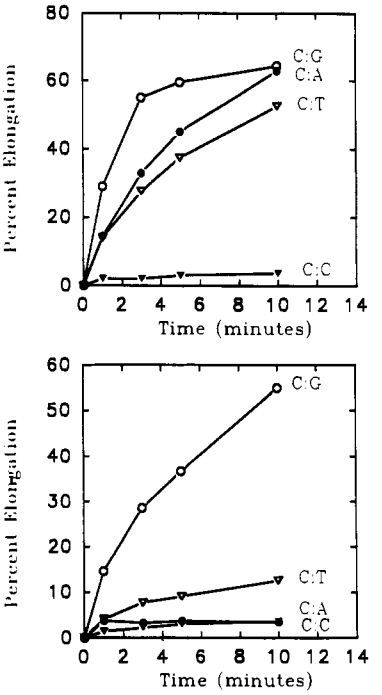

FIGURE 12: Elongation efficiency of various bases incorporated opposite normal cytosine using polI(k)$^{exo-}$ (upper panel) or wild-type polI(k) containing 3′→5′ exonuclease activity (lower panel). Percent elongation was determined as described under Materials and Methods. Values are averages for two experiments.

plex, therefore, mimics a situation in which G, A, T, or C was incorporated opposite εC. DNA synthesis was initiated in the presence of 20 μM dATP, and the products of elongation were fractionated (Figure 10) and quantitated (Figure 11, upper graph) as described. The results demonstrated that the efficiency of εC bypass is strongly affected by the identity of the base incorporated opposite the lesion. Bypass is most efficient when thymine is incorporated opposite εC; it is somewhat less efficient with adenine and very inefficient when guanine or cytosine is present opposite the lesion.

The bypass experiments described above were carried out with polI(k)$^{exo-}$ and therefore do not reveal any additional modulation of bypass mediated by 3′→5′ exonuclease activity normally associated with replication enzymes. Therefore, the above experiments were repeated with wild-type polI(k) containing the 3′→5′ exonuclease activity. The results (Figure 11, bottom graph) showed that although the elongation efficiency was reduced for all εC·N pairs as compared to the efficiency obtained with the exonuclease-deficient enzyme, the most efficiently elongated pair was εC·T. Figure 12 (top graph) shows that on the normal template (25-mer^{C}), the exonuclease-deficient enzyme elongates the C·G base pair as well as C·A and C·T mispairs with relatively high efficiency, whereas the C·C mispair is very poorly elongated. The wild-type enzyme (Figure 12, bottom graph) elongates C·G pairs very efficiently. C·A and C·C mispairs are very poorly elongated. On the other hand, even though C·T elongation is reduced in comparison to that by the mutant enzyme, the C·T mispair is clearly the best elongated of the three mispairs (Figure 12, bottom graph).

Discussion

An advantage of a site-specific adduction approach is the possibility of establishing cause–effect correlations between a defined DNA lesion and a biological or biochemical effect [see review by Basu and Essigmann (1988)]. This approach is most useful when the level of background information on the lesion is sufficient to permit the formulation of highly specific questions, as is the case with εC. As briefly reviewed in the introduction, the observed mutagenic properties of εC may well define a novel type of mutagenic lesion. Therefore, it was deemed important to obtain more definitive evidence for the observed properties. The goal of the experiments described here has been to ask whether εC has the properties of a noninstructional DNA lesion in vitro.

E. coli polI, the model DNA polymerase used in the experiments described here, has the advantages of a well-characterized protein, which is also the most extensively used model polymerase for the study of replication fidelity of damaged templates [see review by Loeb and Kunkel (1982)]. The availability of the 3′→5′-exonuclease-deficient version of polI(k) makes this enzyme particularly useful for examining misinsertion opposite noninstructional lesions as described here. The mutant version appears to differ from the wild-type enzyme only in the 3′→5′ exonuclease activity. The two enzyme species are similar in protein conformation (Derbyshire et al., 1988) and base selectivity during polymerization (Bebenek et al., 1990).

The data presented in this paper make it clear that εC lesions indeed have the properties of noninstructional DNA lesions. Specifically, no base incorporation is observable opposite εC under conditions where normal cytosine is readily replicated. At high nucleotide precursor concentrations, base incorporation follows the patterns established for canonical noninstructional lesions: i.e., a preference for adenine followed by thymine and other bases. This order of incorporation preference is the same whether εC is the first base that must be replicated or whether εC is encountered during elongation (Figure 8).

In this experimental system, even though adenine is favored for incorporation opposite εC, continued elongation (bypass) is more efficient when thymine is incorporated opposite the lesion regardless of whether 3′→5′ exonuclease activity is present. While we have not yet analyzed this phenomenon in detail, the preferential thymine elongation may be specific

to the experimental system (i.e., the sequence context, the enzyme, etc.) rather than to the lesion. Such a possibility is supported by the observation that on the normal template the elongation efficiency of the C·T mispair is higher than that for C·A and C·C mispairs (Figure 12, bottom graph). We are currently examining the kinetics of base incorporation and extension opposite εC by polI by procedures described by Goodman and co-workers (Randall et al., 1987).

ACKNOWLEDGMENTS

We gratefully acknowledge the generous gift of polymerases by Dr. M. Modak and of highly purified dGTP by Dr. N. Sinha.

REFERENCES

Barbin, A., & Bartsch, H. (1986) in *The Role of Cyclic Nucleic Acid Adducts in Carcinogenesis and Mutagenesis No. 70*, pp 345–358, International Agency for Research on Cancer, Lyon, France.

Barbin, A., Bartsch, K., Leconte, P., & Radman, M. (1981) *Nucleic Acids Res. 9*, 375–387.

Barbin, A., Besson, F., Perrard, M.-H., Bereziat, J.-C., Kaldor, J., Michel, G., & Bartsch, H. (1985) *Mutat. Res. 152*, 147–156.

Barrio, J. R., Secrist, J. A., III, & Leonard, N. J. (1972) *Biochem. Biophys. Res. Commun. 46*, 597–604.

Basu, A. K., & Essigmann, J. M. (1988) *Chem. Res. Toxicol. 1*, 1–18.

Bebenek, K., Joyce, C. M., Fitzgerald, M. P., & Kunkel, T. A. (1990) *J. Biol. Chem. 265*, 13878–13887.

Biernat, J., Ciesiolka, J., Gornicki, P., Krzyzosiak, W. J., & Wiewiorowski, M. (1978) *Nucleic Acids Res. 5*, 789–804.

Derbyshire, V., Fremont, P. S., Sanderson, M. R., Beese, L., Friedman, J. M., Joyce, C. M., & Steitz, T. A. (1988) *Science 240*, 199–201.

Eberle, G., Barbin, A., Laib, R. J., Ciroussel, F., Thomale, J., Bartsch, H., & Rajewsky, M. F. (1989) *Carcinogenesis 10*, 209–212.

Green, T., & Hathaway, D. E. (1978) *Chem.-Biol. Interact. 22*, 211–224.

Guengerich, F. P., Crawford, W. M., Jr., & Watanabe, P. G. (1979) *Biochemistry 18*, 5177–5182.

Hall, J. A., Saffhill, R., Green, T., & Hathaway, D. E. (1981) *Carcinogenesis 2*, 141–146.

Hollstein, M., Nair, J., Bartsch, H., Bochner, B., & Ames, B. N. (1986) in *The Role of Cyclic Nucleic Acid Adducts in Carcinogenesis and Mutagenesis No. 70*, pp 437–448, International Agency for Research on Cancer, Lyon, France.

Jacobsen, J. S., & Humayun, M. Z. (1990) *Biochemistry 29*, 496–504.

Jacobsen, J. S., Refolo, L. M., Conley, M. P., Sambamurti, K., & Humayun, M. Z. (1987) *Mutat. Res. 179*, 89–101.

Jacobsen, J. S., Perkins, C. P., Callahan, J. T., Sambamurti, K., & Humayun, M. Z. (1989) *Genetics 121*, 213–222.

Kochetkov, N. K., Shibaev, V. N., & Kost, A. A. (1971) *Tetrahedron Lett. 22*, 1993–1996.

Kohwi-Shigematsu, T., Gelinas, R., & Weintraub, H. (1983) *Proc. Natl. Acad. U.S.A. 80*, 4389–4393.

Krzyzosiak, W. J., Wiewiorowski, M., & Jaskolski, M. (1986) in *The Role of Cyclic Nucleic Acid Adducts in Carcinogenesis and Mutagenesis No. 70*, pp 75–81, International Agency for Research on Cancer, Lyon, France.

Kunkel, T. A. (1984) *Proc. Natl. Acad. Sci. U.S.A. 81*, 1494–1498.

Kusmierek, J. T., & Singer, B. (1982) *Biochemistry 21*, 5717–5722.

Laib, R. J., & Bolt, H. M. (1977) *Toxicology 8*, 185–195.

Leithauser, M. T., Liem, A., Stewart, B. C., Miller, E. C., & Miller, J. A. (1990) *Carcinogenesis 11*, 463–473.

Leonard, N. J. (1984) *CRC Crit. Rev. Biochem. 15*, 125–199.

Lilley, D. M. J. (1986) in *The Role of Cyclic Nucleic Acid Adducts in Carcinogenesis and Mutagenesis No. 70*, pp 83–99, International Agency for Research on Cancer, Lyon, France.

Loeb, L. A., & Kunkel, T. A. (1982) *Annu. Rev. Biochem. 52*, 429–457.

Loeb, L. A., & Preston, B. D. (1986) *Annu. Rev. Genet. 20*, 201–230.

McCann, J., Simon, V., Streitweiser, D., & Ames, B. N. (1975) *Proc. Natl. Acad. Sci. U.S.A. 72*, 3190–3193.

Rabkin, S. D., & Strauss, B. S. (1984) *J. Mol. Biol. 178*, 569–594.

Randall, S. K., Eritja, R., Kaplan, B. E., Petrushka, J., & Goodman, M. F. (1987) *J. Biol. Chem. 262*, 6864–6870.

Randerath, K., Reddy, M. V., & Gupta, R. C. (1981) *Proc. Natl. Acad. Sci. U.S.A. 78*, 6126–6129.

Sambrook, J., Fritsch, E. F., & Maniatis, T. (1989) *Molecular Cloning: A Laboratory Manual*, Cold Spring Harbor Laboratory Press, Cold Spring Harbor, NY.

Shulman, L. H., & Pelka, H. (1976) *Biochemistry 15*, 5769–5775.

Singer, B., & Spengler, S. J. (1986) in *The Role of Cyclic Nucleic Acid Adducts in Carcinogenesis and Mutagenesis No. 70*, pp 359–371, International Agency for Research on Cancer, Lyon, France.

Singer, B., Kusmierek, J. T., & Fraenkel-Conrat, H. (1983) *Proc. Natl. Acad. Sci. U.S.A. 80*, 969–972.

Vogt, N., Marrot, L., Rousseau, N., Malfoy, B., & Leng, M. (1988) *J. Mol. Biol. 201*, 773–776.

Walker, G. C. (1984) *Microbiol. Rev. 48*, 60–93.